View metadata, citation and similar papers at core.ac.uk
brought to you by CORE
provided by Scientific Open-access Literature Archive and Repository

IL NUOVO CIMENTO Vol. 35 C, N. 6 Novembre-Dicembre 2012
DOI 10.1393/ncc/i2012-11358-6

Colloquia: LaThuile12

Recent results on QCD and forward physics from the CMS Collaboration

R. Arcidiacono on behalf of the CMS Collaboration
Università del Piemonte Orientale and INFN - Torino, Italy

ricevuto il 7 Settembre 2012

Summary. — A selection of recent results on QCD, diffraction and exclusive processes from the CMS experiment at LHC are here presented. The measurements refer to data which have been collected in 2010, during proton-proton collisions at the center-of-mass energy of $\sqrt{s} = 7$ TeV. The results rely on excellent performance of the tracking systems as well as on unprecedented calorimetry pseudo-rapidity coverage.

PACS 12.38.Qk – Quantum chromodynamics: Experimental tests.
PACS 13.85.-t – Hadron-induced high- and super-high-energy interactions (energy > 10 GeV).

1. – Introduction

LHC is the highest-energy proton-proton collider and, at the same time, the machine where the lowest parton momentum fraction, ξ, can be achieved, allowing the exploration of new regions of the parton dynamics phase space. This machine provides excellent and unique opportunities to tune Monte Carlo generators and test the validity of QCD and Standard Model predictions at high energy, as well as the possibility to study rare processes. All the measurements here presented make use of the data collected in 2010, during proton-proton collisions at the center of mass energy of $\sqrt{s} = 7$ TeV. For most of them, the low pile-up conditions characterizing the 2010 data taking represent the best environment to perform precision tests of QCD observables and forward physics processes.

2. – The CMS detector

The CMS detector main component is a 6 m diameter, 13 m long solenoidal magnet, operated to generate a 3.8 T magnetic field. Pixel and silicon strips tracking detectors are located inside the solenoid, with a pseudo-rapidity $|\eta| < 2.5$ coverage. Always inside the

© CERN on behalf of the CMS Collaboration under CC BY-NC 3.0

solenoid and surrounding the tracking systems, there are a lead tungstate crystal electromagnetic calorimeter (ECAL), and a brass-scintillator hadronic calorimeter (HCAL), covering $|\eta| < 2.9$ and < 3.0 regions, respectively. The pseudo-rapidity is defined as $\eta = -\log[\tan(\theta/2)]$, where θ is the polar angle of the particle with respect to the beam axis.

Outside the solenoid and embedded in the return yoke of the magnet, there are several layers of muon chambers composed by drift tubes, resistive plate chambers and cathode strip chambers. They form a high resolution and redundant muon detection system.

CMS is also equipped with Cerenkov calorimeters in the forward region, characterized by a challenging environment due to the limited space and high radiation levels. The hadronic forward calorimeter covers the range $2.9 < |\eta| < 5.2$, the CASTOR calorimeter, located on the minus side, covers the range from 6.6 to 5.2, and the Zero-Degree calorimeter extends the rapidity coverage beyond 8.1 (for neutral particles).

A detailed description of CMS can be found in [1].

3. – QCD results

Among the several measurements which are of great interest as QCD tests and QCD model tunings, we presents the results obtained for the total (visible) proton-proton (pp) inelastic cross section at $\sqrt{s} = 7\,\text{TeV}$, measured with two independent methods covering different phase space, and for the Underlying Event (UE) activity. Both measurements are important for precision tests of Standard Model processes and new physics searches.

3˙1. *Inelastic proton-proton cross section measurement.* – CMS has performed the measurement of the visible inelastic proton-proton cross section with two independent methods that make use of the central tracking system and of the hadronic forward calorimeters [2, 3]. The calorimeter-based technique is especially sensitive to low-mass states, boosted along the beam line, but might miss central diffractive events, while the track method accounts for the events with central activity and does not cover high rapidity events.

The track-based method makes use of the pile-up events (interactions which occur at the same time of a given triggered bunch crossing) distributions, present during standard 2010 data taking, and relies on the high performance of the tracking system. The technique is the following: in single-μ events, the distribution of extra vertexes is measured, in bins of instantaneous luminosity, separately for events having between one and nine vertexes; the distributions obtained are corrected for the vertex reconstruction efficiency; the visible cross section σ_{pp} is derived by fitting the corrected vertex distributions, assuming that the probability of having n pile-up events is given by the Poisson law:

$$P(n) = \frac{(L \cdot \sigma_{pp})^n}{n!} e^{-L \cdot \sigma} \tag{1}$$

as a function of the instantaneous luminosity L.

This technique is repeated for three different categories of visible events, characterized by having at least 2, 3 or 4 tracks with $|\eta| < 2.4$ and $p_T > 200\,\text{MeV}$. For each category, the visible cross section measurement is referred to the corresponding hadron-level definition which requires at least 2, 3 or 4 generated charged particles with $|\eta| < 2.4$ and $p_T > 200\,\text{MeV}$. The acceptance and reconstruction efficiency correction is derived from the CMS detector simulation and it is totally model-independent. Figure 1 shows

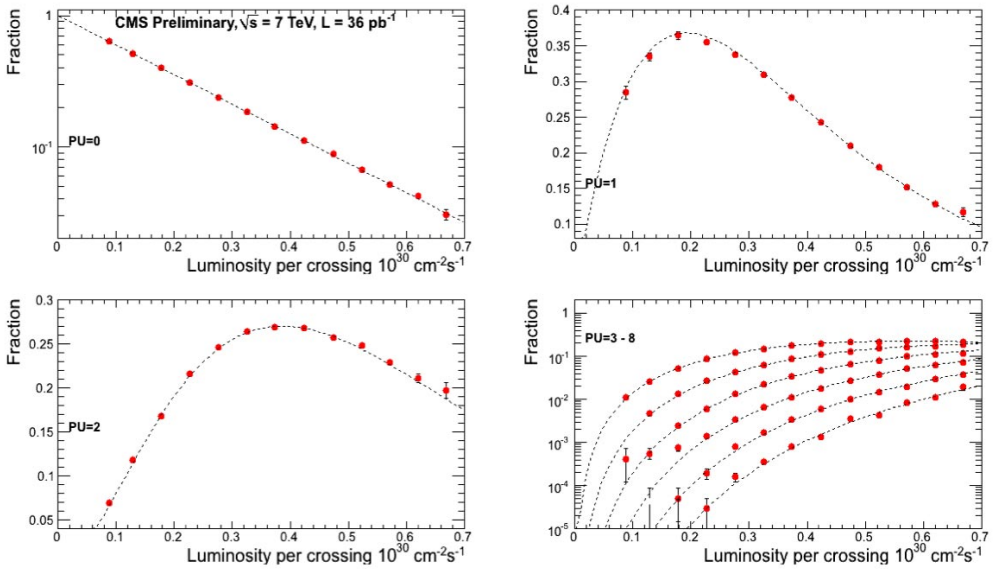

Fig. 1. – Fraction of events with > 1 track with pile-up events = 0–8 as a function of luminosity. The dotted lines are Poisson fits.

the comparison of the distribution of vertexes in the data (for events with at least two tracks) and in the MC, as a function of the instantaneous luminosity, for pile up from 0 to 8. The main source of systematic uncertainty is the error on the CMS luminosity determination, which is 4%. The systematic checks performed include the usage of a different dataset, the study of dependency upon the fit parameters, vertex reconstruction quality and efficiency corrections.

The measured values of σ_{pp}, for events with at least 2, 3 or 4 charged particles with $|\eta| < 2.4$ and $p_T > 200\,\text{MeV}$, and their systematic errors are

$$\begin{aligned}
\sigma_{pp}(> 1\text{track}) &= [58.7 \pm 2.0\ (\text{syst}) \pm 2.4\ (\text{lum})]\ \text{mb},\\
\sigma_{pp}(> 2\text{tracks}) &= [57.2 \pm 2.0\ (\text{syst}) \pm 2.4\ (\text{lum})]\ \text{mb},\\
\sigma_{pp}(> 3\text{tracks}) &= [55.4 \pm 2.0\ (\text{syst}) \pm 2.4\ (\text{lum})]\ \text{mb}.
\end{aligned}$$

In the HF-based method, the number of pp collisions which deposit at least $E = 5\,\text{GeV}$ in either of the HF calorimeters are counted. The threshold of 5 GeV is used to reject a large part of the detector noise still selecting pp collisions with high efficiency. The analysis is performed using events triggered by the Zero-Bias condition (LHC colliding beams in the given bunch crossing), collected during the low luminosity runs with pile up probability ranging between 0.7% and 12%. The number of true pp collisions, which are proportional to the cross section to be measured, are obtained by correcting the measured counting for the selection efficiency, evaluated with Monte Carlo studies, the pile up probability and the detector noise, measured in data with dedicated triggers.

At generator level, the HF activity requirements correspond to selecting events where at least one proton looses more than a fraction $\xi = 5 \times 10^{-6}$ of its momentum. The variable ξ is also defined as $\xi = M_X^2/s$, where s is the squared center-of-mass energy and

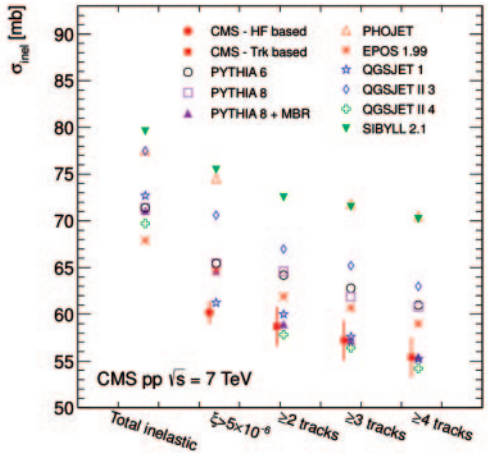

Fig. 2. – Comparison between the CMS measurements of the inelastic pp cross section for the four different final states and the predictions of several Monte Carlo models. Monte Carlo predictions have a common uncertainty of 1 mb (not shown).

M_X is the mass of the higher system in the collision products, which is separated from the rest by the largest rapidity gap in the event (for diffractive events ξ is the fraction of momentum lost by the outgoing proton).

The measured visible cross section for events with $\xi > 5 \times 10^{-6}$ is

$$\sigma_{pp}(\xi > 5 \times 10^{-6}) = [60.2 \pm 0.2\ (\text{stat}) \pm 1.1\ (\text{syst}) \pm 2.4\ (\text{lum})]\ \text{mb},$$

where the systematic uncertainty takes into account the studies performed on selection efficiency, contamination from lower ξ region, HF energy threshold, detector noise effects.

Figure 2 compares the four CMS results with the predictions of several models, from Pythia6, Pythia8 tand Phojet as well as three models, based on the same Regge-Gribov phenomenology as Phojet but with different implementations of various model ingredients, commonly used in cosmic ray physics (Qgsjet, Sybill and Epos).

Phojet and Sybill overestimate the cross section by more than 20%, Epos, Qgsjet (Q-II-03), Pythia6 and Pythia8 tunes are 10% above the measured cross sections, while Qgs01 and Qgsjet (Q-II-04) agree within one standard deviation of the data points.

3˙2. *Underlying event measurements*. – In hadron-hadron scattering the underlying event (UE) is defined as all the processes which can be attributed to the hadronization of the partons involved in the hardest scatter. The underlying event is thus composed by initial- and final-state radiations, the particles produced by the multiple parton interactions (MPI) and the beam-beam-remnants (BBR) resulting from the hadronization of the partonic constituents that did not participate in other scatterings. It is important to measure and model correctly the underlying event for the precision measurements of Standard Model processes and the search for new physics at high energies.

To define observables which are sensitive to the UE activity, after having identified the direction of the leading track or jet (reflecting the hard scatter parton direction), charged particles are categorized according to their azimuthal distance $\Delta\phi$ w.r.t the leading object. The particle production in the away region ($|\Delta\phi| > 120°$) is expected to be dominated by the recoiling partons balancing the hard scatter whereas the transverse region ($60° < |\Delta\phi| < 120°$) should be the best for the study of the underlying event. The strength of the UE activity is measured in terms of the average charged-particle multiplicity and the average scalar sum of p_T of the charged particles, expressed as density dividing by the area of the considered $\eta \times \phi$ space.

CMS has performed the measurement of the underlying event activity at $\sqrt{s} = 0.9$ and 7 TeV [4, 5], in minimum bias events where the hard scatter direction is identified by the leading track-jet (highest p_T object formed using a jet algorithm applied to reconstructed tracks). The track-jet p_T also defines the scale of the event. A strong increase of the UE activity in the transverse region is observed with increasing leading track-jet p_T. In the 7 TeV data, the fast rise is followed by a plateau region, above 8 GeV/c, with nearly constant multiplicity and small Σp_T^{CH} increase, indicating that particle production due to MPI saturates. A strong growth in hadronic activity is also observed as a function of the center-of-mass energy. Several tunes of PYTHIA6 and PYTHIA8 have been compared to the measurements, with a good description of most distributions at 7 TeV and of the dependence from 0.9 to 7 TeV provided by the Z1 tune.

A complementary method to study the underlying event is the one using the well-known Drell-Yan di-muon final state $q\bar{q} \to \mu\mu$, with the di-muon invariant mass in the Z mass range ($60\,\text{GeV} < m_{\mu\mu} < 120\,\text{GeV}$) [6]. In this process it is possible to separate very well the contribution due to the primary hard scatter and the background contamination level is very low. The average charged-particle multiplicity density and the average Σp_T^{CH} density are studied in the three distinct topological regions, away, transverse and towards, defined with respect to the resulting direction of the di-muons system, as a function of di-muon invariant mass and transverse p_T. After excluding the muons of the DY event, the activity in the transverse region is found to be higher than the activity in the towards region due to the spill-over contribution from the hadronic recoil activity in the away region, as shown in fig. 3. The UE activity shows a small growth as a function of $p_T^{\mu\mu}$ mainly due to the increase of radiations, combined with a saturated MPI contribution as the scale of the hard process is high ($\sim M_Z$). These measurements have been compared to predictions of various PYTHIA tunes, PYTHIA6 Z1, PYTHIA6 DW and PYTHIA8 4C. These models differ in the PDF description, in the implementation of initial and final state radiations, fragmentation and the MPI. The average Σp_T^{CH} density is described well by the PYTHIA6 Z1 tune with a maximum discrepancy of 10% at small values of $p_T^{\mu\mu}$, whereas the average charged particle density is in agreement with the prediction of PYTHIA6 Z1 and DW. PYTHIA8 4C predictions show good agreement with the data only at small $p_T^{\mu\mu}$.

4. – Measurement of hard diffraction at LHC

Evidence of hard diffraction at the LHC has been observed in events associated to W and Z boson production with large rapidity gaps (LRG) [7]. In particular, a large asymmetry in the signed pseudo-rapidity (particle charge $\times|\eta|$ distribution) of the W and Z-decay leptons is observed. This asymmetry is well described by the prediction of the POMPYT generator. The diffractive component is determined to be $50.0 \pm 9.3(\text{stat.}) \pm 5.2(\text{syst.})\%$ and provides the first evidence of diffractive W/Z production at the LHC.

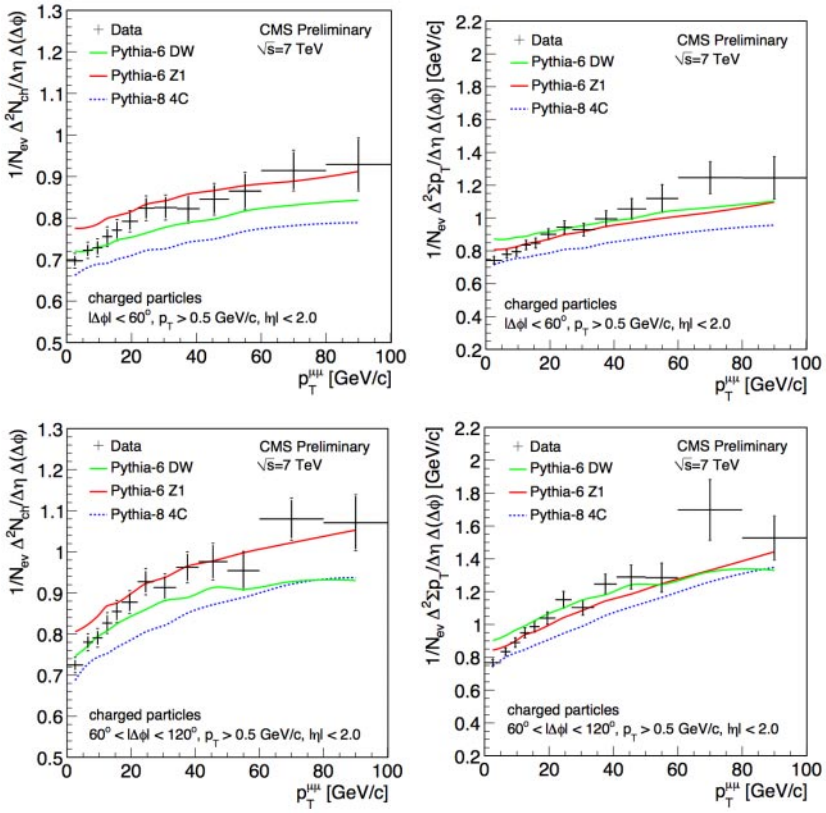

Fig. 3. – Plots on the top (bottom) row show the average charged particle multiplicity and Σp_T^{CH} densities as a function of $p_T^{\mu\mu}$ in the towards (transverse) region, as measured in DY di-muon events after having excluded the two muons.

Another recent result, based on an integrated luminosity of $2.7\,\mathrm{nb}^{-1}$ collected in 2010 with very low pile up conditions, refers to the measurement of single-diffractive di-jet events [8]. The events are selected requiring two jets with transverse momentum $p_T > 20\,\mathrm{GeV}$ in the range $|\eta| < 4.4$. The differential cross section for di-jet production is shown in fig. 4 as a function of the reconstructed ξ, a variable that approximates the fractional momentum loss of one of the scattered protons in single diffractive pp collisions. The results are compared to the predictions of diffractive and non-diffractive Monte Carlo models. The low-ξ events are dominated by diffractive di-jet production.

5. – Exclusive processes at LHC

In central exclusive productions, *i.e.* $pp \to p + X + p$, the colliding protons remain intact with small transverse momentum after an interaction and all the transferred energy goes into a central color singlet system, which is fully measured. No other particles are produced in the interaction and large rapidity gaps are present. Three main types of exclusive process are QED $\gamma\gamma$ interaction (*e.g.*, exclusive $\mu^+\mu^-$, e^+e^- production), γIP fusion (*e.g.*, exclusive Υ production) and IPIP exchange (*e.g.*, exclusive $\gamma\gamma$ or Higgs boson

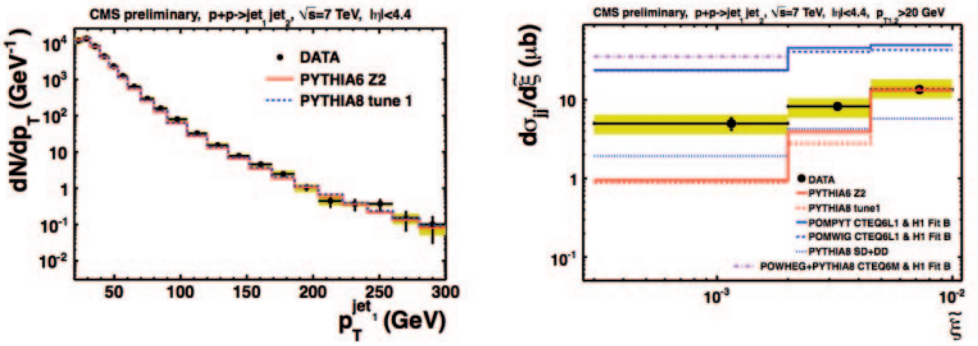

Fig. 4. – On the left: transverse-momentum distribution of the first—highest p_T—jet for data (black points) and non-diffractive MC generators (PYTHIA6 Z2 and PYTHIA8 tune 1). On the right: differential cross section for di-jet events as a function of reconstructed ξ. The predictions of non-diffractive (PYTHIA6 Z2 and PYTHIA8 tune 1) and diffractive (POMPYT SD, POMWIG SD and PYTHIA8 SD+DD) MC generators are also shown.

production), where IP denotes a pomeron. Recent results on exclusive $\gamma\gamma$ production of $\mu^+\mu^-$, e^+e^-, and on the double Pomeron exchange production of $\gamma\gamma$ final states are here presented.

5˙1. *Exlcusive di-muon events.* – A measurement of the exclusive two-photon production of muon pairs, $pp \to p + \mu^+\mu^- + p$ has been performed on the complete 2010 dataset of $40\,\mathrm{pb}^{-1}$ [9]. This QED process has small theoretical uncertainties and striking kinematic distributions, which make it an attractive candidate for absolute calibration of luminosity of pp collisions. Events are selected requiring to have one vertex with only two tracks (muons) associated, within 2 mm; both muons transverse momentum $p_T > 4\,\mathrm{GeV}$ and located in the pseudo-rapidity region $|\eta| < 2.1$. Moreover the di-muon invariant mass has to be greater than 11.5 GeV, to remove the contribution from exclusive photoproduction of upsilon mesons. The exclusivity condition is imposed only on the primary vertex, using the tracking system only. For muon pairs thus selected, a fit to the $p_T(\mu^+\mu^-)$ distribution results in a measured partial cross section of $\sigma = [3.38^{0.58}_{-0.55}(\mathrm{stat.}) \pm 0.16(\mathrm{syst.}) \pm 0.14(\mathrm{lumi})]$ pb. The ratio to the predicted value is $0.83^{0.14}_{0.13}(\mathrm{stat.}) \pm 0.04(\mathrm{syst.})$. The characteristic distributions of the muon pairs produced via $\gamma\gamma$ fusion, such as the muon acoplanarity, the muon pair invariant mass and transverse momentum, are well described by the full detector simulation using the LPAIR event generator.

5˙2. *Search for exclusive di-photon/di-electron events.* – Central exclusive $\gamma\gamma$ and e^+e^- events have been studied in a data sample corresponding to an integrated luminosity of $36\,\mathrm{pb}^{-1}$ [10]. Since an overlapping inelastic pp interaction, in the same beam crossing, would spoil the exclusivity condition and make the exclusive interaction unobservable, only beam crossings with single interactions (no pile-up) are used in this analysis.

The exclusive $\gamma\gamma$ (e^+e^-) event signature requires two reconstructed photon candidates (one positron and one electron candidates), each with transverse energy $E_T > 5.5\,\mathrm{GeV}$ and pseudo-rapidity $|\eta| < 2.5$, and no other particles detected in the range $|\eta| < 5.2$. The incident protons stay intact, or diffractively dissociate, escaping along the beam direction

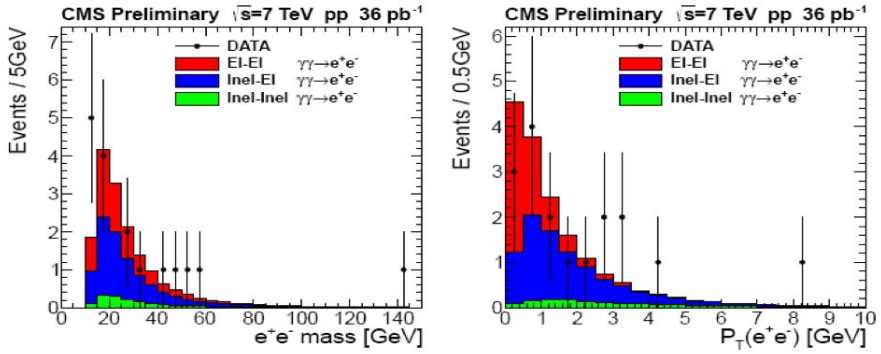

Fig. 5. – Di-electron invariant mass (left) and p_T distributions (right) for the exclusive e^+e^- events, compared to the LPAIR Monte Carlo predictions for the exclusive (El-El) and semi-exclusive (Inel-El, Inel-Inel) categories.

without being detected. The detector noise and beam background have been studied in zerobias and unpaired bunches events.

No di-photon candidate satisfies all the selection criteria. An upper limit on the cross section of $pp \to p + \gamma\gamma + p$ with $E_T(\gamma) > 5.5\,\text{GeV}$ and $|\eta| < 2.5$ is set at 1.30 pb with 95% confidence level.

For the di-electron channel, 17 e^+e^- candidates on a background of 0.84 ± 0.28 (stat.) events are observed. The theoretical QED prediction evaluated with the event generator LPAIR is 16.5 ± 1.7(theo.) $\pm$ 1.2(syst.) events. The semi-exclusive e^+e^- having one or both protons dissociated and escape undetected are here considered as signal. Figure 5 shows the di-electron invariant mass and the p_T distributions, in good agreement with the QED predictions.

REFERENCES

[1] CMS Collaboration, *JINST*, **03** (2008) S08004.
[2] CMS Collaboration, *Measurement of the inelastic pp cross section at* $\sqrt{s} = 7\,\text{TeV}$ *with the CMS detector, Physics Analysis Summary* FWD-11-001 (2011).
[3] CMS Collaboration, *Measurement of the inelastic pp cross section at* $\sqrt{s} = 7\,\text{TeV}$, *Physics Analysis Summary* QCD-11-002 (2011).
[4] CMS Collaboration, *Eur. Phys. J. C*, **70** (2010) 555.
[5] CMS Collaboration, *JHEP*, **09** (2011) 109.
[6] CMS Collaboration, *Measurement of the Underlying Event activity in the Drell-Yan process in proton-proton collisions at* $\sqrt{s} = 7\,\text{TeV}$, *Physics Analysis Summary* QCD-10-040 (2010).
[7] CMS Collaboration, *Forward energy flow and central track multiplicities in W and Z boson events at* $\sqrt{s} = 7\,\text{TeV}$ *pp collisions, Physics Analysis Summary* FWD-10-008 (2010).
[8] CMS Collaboration, *Evidence for hard-diffractive dijet production in pp collisions at* $\sqrt{s} = 7\,\text{TeV}$, *Physics Analysis Summary* FWD-10-004 (2010).
[9] CMS Collaboration, *Measurement of exclusive* $\gamma\gamma \to \mu^+\mu^-$ *production at* $\sqrt{s} = 7\,\text{TeV}$, *Physics Analysis Summary* FWD-10-005 (2011).
[10] CMS Collaboration, *Search for central exclusive* $\gamma\gamma$ *production and observation of central exclusive* e^+e^- *production in pp collisions at* $\sqrt{s} = 7\,\text{TeV}$, *Physics Analysis Summary* FWD-11-004 (2011).